Inorganic Chemistry

Article

The Indium Subnitrides Ae$_6$In$_4$(In$_x$Li$_y$)N$_{3-z}$ (Ae = Sr and Ba)

Mark S. Bailey, Daniel Y. Shen,[†] Michael A. McGuire,[‡] Daniel C. Fredrickson, Brian H. Toby,[§]
Francis J. DiSalvo,* Hisanori Yamane,[∥] Shinya Sasaki,[⊥] and Masahiko Shimada[⊥]

Department of Chemistry and Chemical Biology, Cornell University, Ithaca, New York 14853

Received April 21, 2005

The indium nitrides Sr$_6$In$_4$(In$_{0.32}$Li$_{0.92}$)N$_{2.49}$ and Ba$_6$In$_{4.78}$N$_{2.72}$ have been synthesized from an excess of molten sodium. They crystallize in a stuffed variant of the η-carbide structure type in the cubic space group $Fd\bar{3}m$ with $Z = 8$. The lattice parameters are $a = 14.3752(4)$ and $15.216(1)$ Å, with cell volumes 2970.6(2) and 3523.3(6) Å^3, respectively. In both compounds there are vacancies on some of the indium and nitrogen sites and, in the case of Sr$_6$In$_4$(In$_{0.32}$Li$_{0.92}$)N$_{2.49}$, mixed lithium–indium occupancy of one metal site. It is demonstrated that the partial and mixed occupancies act to carefully tune to electron count to almost fulfill the bonding requirements of the stellar quadrangular subnets of both compounds. Four probe resistivity measurements performed upon a pellet of Sr$_6$In$_4$(In$_{0.32}$Li$_{0.92}$)N$_{2.49}$ show it to have a room-temperature resistivity of 6.3 mΩ·cm with a weak temperature dependence.

Introduction

The binary nitrides of the p-block (M$_x$N$_y$) include boron nitride, silicon nitride, and gallium nitride. The M—N bonds within all three compounds are strong and contain a high degree of covalent character. Furthermore, in bulk form, all three compounds are relatively inert toward oxide formation when heated in air and are very stable in mildly reducing environments; for example, both hexagonal boron nitride and silicon nitride are commercially useful as crucible materials and diffusion barriers, respectively. The intrinsic materials characteristics of GaN are well suited for the high-power semiconductor industry; GaN is a direct, large band gap semiconductor ($E_g = 3.4$ eV[1]) with a small unit cell, moderately strong gallium—nitrogen bonds, and high carrier mobility.

As the p-block metal, M, becomes heavier, the M—N bond strength decreases considerably;[2–4] for example, indium

nitride (InN, $E_g = 0.7$ eV[1]) adopts the same wurtzite structure type as gallium nitride but the standard heat of formation of indium nitride is −28.6 kJ/mol[2], considerably less than that of gallium nitride, −156.8 kJ/mol[2]. This difference in strength between the Ga—N and In—N bond results in an interesting schism in the structures and numbers of the alkaline-earth (Ae) containing compounds, Ae$_x$M$_y$N$_z$ (M = Ga or In). There are almost twice as many reported Ae$_x$Ga$_y$N$_z$[5–13] compounds than Ae$_x$In$_y$N$_z$ compounds,[13–18] and in the majority of the ternary gallium nitrides, the formal oxidation state of the gallium is either I or III; i.e., it is formally a positive cation.

---

* To whom correspondence should be addressed. E-mail: fjd3@cornell.edu.

† Current address: School of Medicine, New York University, New York, NY 10016.

‡ Department of Physics, Cornell University, Ithaca, NY 14853.

§ NIST Center for Neutron Research, National Institute of Standards and Technology, Gaithersburg, MD 20899-8563.

∥ Institute for Interdisciplinary Research, Tohoku University, 6-3 Aramaki, Aoba-ku, Sendai 980-8578, Japan.

⊥ Institute for Multidisciplinary Research for Advanced Materials, Tohoku University, 2-1-1 Katahira, Aoba-ku, Sendai 980-8577, Japan.

(1) Yu, K. M.; Liliental-Weber, Z.; Walukiewicz, W.; Shan, W.; Ager, J. W., III; Li, S. X.; Jones, R. E.; Haller, E. E.; Lu, H.; Schaff, W. J. *Appl. Phys. Lett.* **2005**, *86*, 071910-1−071910-3.
(2) Ranade, M. R.; Tessier, F.; Navrotsky, A.; Marchand, R. *J. Mater. Res.* **2001**, *16* (10), 2824−2831.
(3) DiSalvo, F. J.; Clarke, S. J. *Curr. Opin. Solid State Mater Sci.* **1996**, *1* (2), 241−249.
(4) Gregory, D. H. *Dalton Trans.* **1999**, *3*, 259−270.
(5) Yamane, H.; DiSalvo, F. J. *Acta Crystallogr.* **1996**, *C52*, 760−761.
(6) Cordier, G.; Höhn, P.; Kniep, R.; Rabenau, A. *Z. Anorg. Allg. Chem.* **1990**, *591*, 58−66.
(7) Park, D. G.; Gál, Z. A.; DiSalvo, F. J. *Inorg. Chem.* **2003**, *42* (5), 1779−1785.
(8) Clarke, S. J.; DiSalvo, F. J. *J. Alloys Compd.* **1998**, *274*, 118−121.
(9) Clarke, S. J.; DiSalvo, F. J. *Inorg. Chem.* **1997**, *36*, 1143−1148.
(10) Cordier, G. *Z. Naturforsch.* **1988**, *43b*, 1253−1255.
(11) Verdier, P.; L'Haridon, P.; Maunaye, M.; Marchand, R. *Acta Crystallogr.* **1974**, *B30*, 226−228.
(12) Cordier, G.; Ludwig, M.; Stahl, D.; Schmidt, P. C.; Kniep, R. *Angew. Chem., Int. Ed. Engl.* **1995**, *34* (16), 1761−1763.
(13) Höhn, P.; Ramlau, R.; Rosner, H.; Schnelle, W.; Kniep, R. *Z. Anorg. Allg. Chem.* **2004**, *630*, 1704.
(14) Kirchner, M.; Wagner, F. R.; Schnelle, W.; Niewa, R. *Z. Anorg. Allg. Chem.* **2004**, *630*, 1735.
(15) Bailey, M. S.; DiSalvo, F. J. *J. Alloys Compd.* **2003**, *353*, 146−152.
(16) Cordier, G.; Rönninger, S. *Z. Naturforsch.* **1987**, *42b*, 825−827.
(17) Yamane, H.; Sasaki, S.; Kajiwara, T.; Yamada, T.; Shimada, M. *Acta Crystallogr.* **2004**, *E60*, i120−i123.
(18) Schlechte, A.; Prots, Yu.; Niewa, R. *Z. Kristallogr.—New Cryst. Struct.* **2004**, *219*, 349−350.

Indium Subnitrides $Ae_6In_4(In_xLi_y)N_{3-z}$

In all the reported $Ae_xIn_yN_z$ compounds, such as Ca_{19}-In_8N_7,[14] Ca_2InN,[15] and $Ba_{19}In_9N_9$,[17] there is insufficient nitrogen to fully oxidize the metals; indeed, the formal oxidation state of the indium is negative and indium−indium bonding is apparent. Gallium−gallium bonding occurs only in $Ca_5Ga_2N_4$[10] and $CaGaN$,[11] the two $Ae_xGa_yN_z$ compounds that contain Ga(I), and in the few compounds that contain anionic gallium, $(Ae_6N)Ga_5$ (Ae = Sr, Ba)[12] and Ca_7-$Ga_{1+\delta}N_4$.[13] However, the most significant difference between the ternary indium and gallium nitrides is that none of the $Ae_xIn_yN_z$ compounds exhibit direct indium−nitrogen bonds. In only $Ca_7Ga_{1+\delta}N_4$,[13] which is isotypic to $Ca_7In_{1+\delta}N_4$,[13] and $(Ae_6N)Ga_5$ (Ae = Sr, Ba)[12] are there no gallium−nitrogen bonds. Direct indium−nitrogen bonding is also absent in all of the known multinary indium nitrides such as $Sr_8Cu_3In_4$-N_5[19] and R_3InN[20] (R = Ti,[21] Sc, La−Nd, Sm, Gd−Tm, Lu). In fact, the only known nitrides to contain a direct indium−nitrogen bond are InN and its solid solutions with gallium nitride, $In_{1-x}Ga_xN$;[22] however, indium−nitrogen bonds are apparent in the cyanamides $In_{2.24}(NCN)_3$ and $NaIn(NCN)_2$.[23]

The NaBa[24] and Ti_2Ni[25] structures are closely related. Both are cubic, space group $Fd\bar{3}m$, and contain 96 atoms in the unit cell. The atoms occupy the same three Wyckoff positions, namely the 48f, the 32e, and the 16d sites (using assignments with the origin at $\bar{3}m$, origin setting 2). In both compounds, the 48f and the 32e sites are occupied by different elements and it is the nature of the atom that occupies the 16d site that determines the different atomic ratios of NaBa and Ti_2Ni. In the NaBa structure, the sodium atoms occupy the 32e and 16d sites and the barium atoms the 48f sites. In Ti_2Ni the nickel atoms occupy only the 32e sites and the titanium atoms occupy both the 48f and 16d sites.

The distribution of the 16d, 32e, and 48f sites in the NaBa and Ti_2Ni structures can be visualized in terms of two distinct subnets. The 32e and 16d sites generate a framework of corner-sharing stellae quadrangulae or tetracapped tetrahedra, an example of which is shown in Figure 1. The 48f sites create a three-dimensional network of face-sharing octahedra that define two distinct vacancies at their centers, at the 16c and 8a positions. Occupation of the 16c site within the octahedral network leads to the η-carbide (W_3Fe_3C) structure type,[26] in which the tungsten atoms form the octahedra and the carbon atoms occupy the octahedral 16c site, within these tungsten octahedra. The iron atoms fill the 32e and 16d sites, forming the net of stellae quadrangulae. Interestingly, the η-carbide structure type is also quite common for mixed
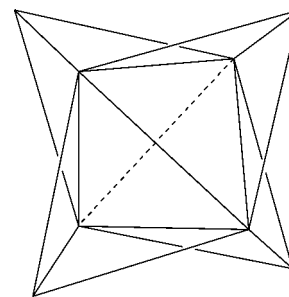

Figure 1. Stella quadrangula formed from capping every tetrahedral face of an inner tetrahedron.

transition-metal nitrides such as Co_3Mo_3N[27] and Fe_4W_2N,[28] in which the nitrogen atoms occupy the octahedral 16c sites.

The crystal orbital overlap population (COOP)[29] and the very closely related crystal orbital Hamilton population (COHP) analyses[30] are very useful electronic structure tools. Both analyses yield information about the bonding or antibonding nature of pairwise interactions in solids. They thus allow the local bonding interactions of an extended solid to be isolated and analyzed. Just as in molecules, these interactions can be bonding or antibonding and, as noted by Dronskowski,[31] nature always attempts to maximize the filling of bonding states and to minimize the filling of antibonding states. This can be achieved in various ways, and it often leads to unusual structural features or physical properties. For example, the ferromagnetism of itinerant electrons in iron, cobalt, and nickel can be explained via spin-polarized COHP analysis.[31] In another study, COOP analysis makes apparent the source of the decreasing lattice parameter in the series of compounds Ti_4TBi_2 (T = Cr, Mn, Fe, Co, and Ni), a decrease larger than that expected from the change of size of the T atom. The COOP analysis revealed that although the Ti−Bi interactions remain strong throughout the series, the T−T bonding increases as the extra electrons funnel into the d−d bonding of these elements.[32] Hence the contraction of the lattice parameter has a physical *and* an electronic root.

In this paper we introduce the isostructural compounds $Sr_6In_4(In_{0.32}Li_{0.92})N_{2.49}$ and $Ba_6In_{4.78}N_{2.72}$. As will be seen, in both compounds there are considerable vacancies at both an indium and a nitrogen site. Furthermore, in $Sr_6In_4(In_{0.32}Li_{0.92})$-$N_{2.49}$, the partially occupied indium site is, in fact, statistically occupied by both indium and lithium. Fully occupied positions would equalize the metal ratio and would result in a structure similar to that of NaBa. The partial (and mixed) occupancies of $Sr_6In_4(In_{0.32}Li_{0.92})N_{2.49}$ and $Ba_6In_{4.78}N_{2.72}$ are explained with the use of electronic structure calculations, especially COOP analyses of the indium subnet.

(19) Yamane, H.; Sasaki, S.; Kubota, S.; Shimada, M.; Kajiwara, T. *J. Solid State Chem.* **2003**, *170*, 265−272.
(20) Kirchner, M.; Schnelle, W.; Wagner, F. R.; Niewa R. *Solid State Sci.* **2003**, *5*, 1247−1257.
(21) Jeitschko, W.; Nowotny H.; Benesovsky, F. *Monatsh. Chem.* **1964**, *95*, 436−438.
(22) See for example: Chang, C.-A.; Shih, C.-F.; Chen, N.-C.; Lin, T. Y.; Liu, K.-S. *Appl. Phys. Lett.* **2004**, *85* (25), 6131−6133.
(23) Dronskowski, R. *Z. Naturforsch.* **1995**, *50b*, 1245−1251.
(24) Snyder, G. J.; Simon, A. *Dalton Trans.* **1994**, *7*, 1159−1160.
(25) Yurko, G. A.; Barton, J. W.; Parr, J. G. *Acta Crystallogr.* **1959**, *12*, 909−911.
(26) Hyde, B. G.; Andersson, S. *Inorganic Crystal Structures*; John Wiley and Sons: New York, 1989.

(27) Jackson, S. K.; Layland, R. C.; zur Loye, H.-C. *J. Alloys Compd.* **1999**, *291*, 94−101.
(28) Weil, K. S.; Kumta, P. N. *J. Solid State Chem.* **1997**, *134*, 302−311.
(29) Hoffmann, R. *Solids and Surfaces: A Chemist's View of Bonding in Extended Structures*; Wiley-VCH: New York, 1988.
(30) Dronskowski, R.; Blöchl, P. E. *J. Phys. Chem.* **1993**, *97*, 8617−8624.
(31) Dronskowski, R. *Int. J. Quantum Chem.* **2004**, *96*, 89−94.
(32) Rytz, R.; Hoffmann, R. *Inorg. Chem.* **1999**, *38*, 1609−1617.

Experimental Section

Due to the reactivity of both the reagents and products with water vapor and oxygen, all manipulations for both compounds were carried out in an argon-filled glovebox unless otherwise stated.

$Sr_6In_4(In_{0.32}Li_{0.92})N_{2.49}$. Two initial reactions were performed. In both cases Na (Aldrich, ACS reagent grade), 200 mg, Sr (filed from rod), 88 mg, In (99.9%), 70 mg, and NaN_3 (99.9%), 70 mg (atomic ratios of $Na:Sr:In:N_2 = 16.0:1.6:1:2.6$), were loaded into a niobium tube (internal volume $\approx 5.4 \times 10^{-6}$ m^3). A 3.5 mg amount of Li (99.9%) (atomic ratio $In:Li::1:0.8$) was also added to the first tube. The niobium containers were sealed under 0.1 MPa of argon in a Centorr Associates arc furnace and then were themselves sealed under vacuum in fused silica tubes, to protect the niobium from oxidation during heating. These starting materials were heated to 800 °C in 15 h, they remained at that temperature for 24 h, and they were linearly cooled to 200 °C over 200 h, at which point the furnace was shut off and allowed to cool naturally. Upon completion of the reactions, unreacted sodium was removed by sublimation from the products by heating the niobium tubes to 350 °C under a pressure of approximately 10^{-1} Pa for 8 h.

The products of the reactions were analyzed with powder X-ray diffraction (XRD) using a Scintag $\theta-\theta$ diffractometer with copper Kα radiation. The samples were prepared for analysis in an argon filled glovebox and covered with Mylar film to prevent aerial oxidation. As analyzed by powder X-ray diffraction (XRD), the products of the two tubes were different, q.v. Results and Discussion. The contents of the lithium-containing tube warranted further analysis; therefore, a sample was removed for single-crystal XRD analysis. Single-crystal X-ray data were collected with Mo Kα radiation on a Bruker SMART CCD equipped with a graphite monochromator. The Bruker software package SAINT[33] was used to integrate the data, an empirical absorption correction[34] was applied, and the files for SHELX[35] were prepared by XPREP.[36] The indium and strontium atoms were found by direct methods, and the nitrogen sites were subsequently found from the Fourier difference map. It was not possible to locate any lithium atoms. The suite of programs within WinGX[37] was also used for further refinement and analysis.

The elemental composition of the crystals was elucidated by electron microprobe analysis using a JEOL 8900 electron microprobe. To prevent decomposition or oxygen contamination of the samples, they were transferred from an argon-filled glovebox to the microprobe in a specially designed portable antechamber that avoids any air exposure during transferral.[38]

Multiple sealed tube reactions between $7Na:1.4Sr:1In:0.4Li:1.6N_2$ provided a bulk sample of $Sr_6In_4(In_{0.32}Li_{0.92})N_{2.49}$ for neutron diffraction and transport measurements. The Sr:In ratio in these reactions was fixed to be the same as observed in the microprobe analysis of the single crystals. A small amount of lithium was also included in these reactions because although lithium had not been observed within the single-crystal X-ray solution, it was an essential reagent for the formation of $Sr_6In_4(In_{0.32}Li_{0.92})N_{2.49}$. An example reaction mixture is Na (Aldrich, ACS reagent grade), 266 mg, Sr (filed from rod), 234 mg, In (99.9%), 217 mg, Li (99.9%), 5 mg,

and NaN_3 (99.9%), 130 mg, which were loaded into a niobium tube (internal volume $\approx 8.1 \times 10^{-6}$ m^3), sealed, and heated in a manner identical with the initial reactions outlined above, except that the slow cooling step was eliminated; i.e., after 24 h at temperature, the furnace was shut off and allowed to cool naturally. Following the reaction, the sodium was removed as described above. The powder XRD pattern from each reaction was identical, and therefore, the products were combined into one bulk sample which was thoroughly mixed. All but three peaks in the powder XRD pattern of this bulk sample could be indexed upon the unit cell of $Sr_6In_4(In_{0.32}Li_{0.92})N_{2.49}$. The intensity of each of the three impurity peaks is $\approx 5\%$ of the most intense $Sr_6In_4(In_{0.32}Li_{0.92})N_{2.49}$ peak. One peak can be assigned to indium, but both of the other two can be assigned to either SrO or Sr_4In_2N; the impurity peaks are too broad to be unambiguously assigned.

When using gaseous reagents in sealed environments, it is prudent to perform simple ideal gas law calculations to ascertain the pressures involved in the reactions. A 130 mg amount of NaN_3 provides approximately 3 mmol of N_2, which, at 800 °C and in a volume of 8.1×10^{-6} m^3, corresponds to a dinitrogen pressure of 3.2 MPa; at temperatures less than 900 °C, it is reasonable to assume that very little nitrogen reacts with the niobium tube.[39] If all the strontium and indium present in the tubes formed $Sr_6In_4(In_{0.32}Li_{0.92})N_{2.49}$, the remaining dinitrogen in the tube would correspond to a pressure of approximately 2.2 MPa at 800 °C; in general, it is found that the niobium tubes can withstand approximately 3−3.5 MPa at temperatures <1000 °C, without bursting or leaking.

Neutron diffraction was performed upon a 2.05 g sample of $Sr_6In_4(In_{0.32}Li_{0.92})N_{2.49}$ which had been loaded into a vanadium container (length 50 mm, inner diameter 9.2 mm) inside a dry helium-filled glovebox and sealed with an indium gasket. The sample holder was sealed in a vacuum cryostat, and a closed-cycle helium refrigerator was used for temperature control. Neutron powder diffraction data were collected at 173 K (the same temperature as the single-crystal data collection) using the BT-1 32 detector neutron powder diffractometer at the NCNR, NBSR. A Cu(311) monochromator with a 90 ° takeoff angle, $\lambda = 1.5402$-(2) Å, and in-pile collimation of 15 min of arc were used. Data were collected over the range of 9−148° in 2θ with a step size of 0.05° in 2θ. The instrument is described in the NCNR WWW site (http://www.ncnr.nist.gov/). Following data collection, a full profile Rietveld analysis of the data was carried out with the programs GSAS[40] and EXPGUI[41] and the single crystal-derived unit cell and atomic coordinates were used as the starting model, including the placement of N1 on the 32e site with 50% occupancy.

A four-probe resistivity measurement was carried out on a 400 mg pellet of $Sr_6In_4(In_{0.32}Li_{0.92})N_{2.49}$. This pellet was prepared by pressing the powder and heating at 600 °C for 150 h in a niobium tube (internal volume $\approx 22.1 \times 10^{-6}$ m^3). A 65 mg amount of sodium azide was also added to provide a dinitrogen atmosphere of approximately 0.5 MPa at the reaction temperature. The sodium was subsequently removed via sublimation by heating to 350 °C under a pressure of ca. 10^{-1} Pa for 8 h. $Sr_6In_4(In_{0.32}Li_{0.92})N_{2.49}$ is extremely air and moisture sensitive, and because of this, the cylindrical pellet was not cut into a rectangular shape before loading into a home-built, airtight sample holder that provides four contacts

(33) *SAINT Plus, Software for the CCD System*; Bruker Analytical X-ray System: Madison, WI, 1999.

(34) Sheldrick, G. M. *SADABS*; Institute für Anorganische Chemie der Universität Göttingen: Göttingen, Germany, 1999.

(35) Sheldrick, G. M. *SHELXL*; Institute für Anorganische Chemie der Universität Göttingen: Göttingen, Germany, 1999.

(36) *XPREP*; Bruker Analytical X-ray Systems: Madison, WI, 1999.

(37) Farrugia, L. J. *J. Appl. Crystallogr.* **1999**, *32*, 837−838.

(38) Ehrlich, G. M. Ph.D. Thesis, Cornell University, Ithaca, NY, 1995.

(39) Reckeweg, O.; Lind, C.; Simon, A.; DiSalvo, F. J. *J. Alloys Compd.* **2004**, *384*, 98−105.

(40) Larson, A. C.; Von Dreele, R. B. *General Structure Analysis System (GSAS)*; Los Alamos National Laboratory Report LAUR 86-748; Los Alamos National Laboratory: Los Alamos, NM, 2000.

(41) Toby, B. H. EXPGUI, a graphical user interface for GSAS. *J. Appl. Crystallogr.* **2001**, *34*, 210−221.

to the sample via four gold pressure pins, as previously described.[42] The resistance of the pellet was measured from 5 to 299 K in 2 K increments. To convert the measured resistance to resistivity, a geometrical factor is required. This was obtained by measuring the room-temperature resistance of an aluminum slug of the same dimensions as the $Sr_6In_4(In_{0.32}Li_{0.92})N_{2.49}$ pellet and comparing it to 2.74 $\mu\Omega\cdot$cm, the literature value at 295 K.[43] The pellet of $Sr_6In_4(In_{0.32}Li_{0.92})N_{2.49}$ was returned to the glovebox after the resistivity measurements, ground up, and analyzed with powder XRD in a manner identical with that described above.

$Ba_6In_{4.78}N_{2.72}$. Ba (99.99%), In (99.999%), and Na (99.95%), in a Ba:In:Na atomic ratio of 2:1:6, were weighed and loaded in a BN crucible (inside diameter 7 mm, height 37.5 mm, 99.5%). The crucible was placed into a stainless steel container (1/2 in. outer diameter) and sealed under argon gas, and the whole assembly was connected to a nitrogen gas feed line. A schematic illustration of the stainless steel container was shown in a previous paper.[44] After heating the sample to 750 °C in an electric furnace, nitrogen gas (>99.9999%) was introduced into the container and the pressure was maintained at 7 MPa with a pressure regulator. The sample was heated at this temperature for 1 h and then cooled to 550 °C at a rate of 2 °C/h under 7 MPa of nitrogen gas. Below 550 °C, the sample was cooled to room temperature in the furnace by shutting off the furnace power. The products in the crucible were washed in liquid ammonia (99.999%) to dissolve away the sodium flux. The details of the sodium extraction procedure were described previously.[45]

To verify the elemental composition of $Ba_6In_{4.78}N_{2.72}$, a handpicked sample of $Ba_6In_{4.78}N_{2.72}$ crystals was dissolved in 1.3 mol/L of HNO_3 solution and the Ba and In ratio was measured by ICP emission spectroscopy (Perkin-Elmer OPTIMA3300).

Electronic Structure Calculations. The electronic structures of both title compounds were investigated with the program YAeH-MOP.[46] The unit cell dimensions of $Ba_6In_{4.78}N_{2.72}$ (i.e. $a = 10.7597$ Å, $\alpha = 60°$) and orbital energies and exponents from ref 47 were used to calculate the COOP curve shown in Figure 5b. All other calculations (including those in the Supporting Information) were performed using the atomic coordinates and unit cell dimensions of $Sr_6In_4(In_{0.32}Li_{0.92})N_{2.49}$ (i.e. $a = 10.152$ Å, $\alpha = 60°$) using Slater type orbitals with the default settings of the energies and exponents. Average property calculations were carried out with a set of 60 k points, and band structures were calculated with 40 points between special positions. All the energies and exponents are listed in the Supporting Information, Table S1.

Results and Discussion

$Sr_6In_4(In_{0.32}Li_{0.92})N_{2.49}$. The two initial reactions that differed only in the presence or absence of lithium had important consequences because the powder XRD patterns of their products were completely different. Following the removal of sodium via sublimation, the lithium-free mixture

yielded a gray, crystalline product whose powder XRD pattern consisted of many peaks, most of which could be assigned to Sr_4In_2N and $SrIn_2$ and none of which could be indexed to $Sr_6In_8(In_{0.32}Li_{0.92})N_{2.49}$. The removal of sodium from the lithium-containing reaction mixture by sublimation yielded a mass of highly crystalline, silvery-yellow bodies and the peaks in the powder XRD pattern could not be matched to any known phase, but all could be indexed upon a cubic cell of $a = 14.4026(2)$ Å. A unit cell of this dimension could not be found in any of our databases, and therefore, some of these silvery-yellow crystals were placed into polybutene oil for optical inspection and single crystal selection.

Optical inspection of the sample in oil showed it to consist of opaque, black polyhedral crystals and black plate crystals. Several of both types of crystal were loaded onto the goniometer head so that a stream of cold nitrogen froze the polybutene oil and held the crystals stationary and protected from the air. The black, platelike crystals gave unit cells that were very similar to that of Li_4SrN_2,[48] but this compound must have been present in concentrations less than a few percent as its peaks were not readily visible in the powder XRD pattern of the bulk sample. The single-crystal diffraction peaks of the opaque, black, polyhedral crystals collected at 173 K could be indexed by a face centered cubic cell with $a = 14.3572(7)$ Å, which is, as expected, slightly smaller than the cell found from the analysis of the room-temperature powder XRD data. A suitable multifaceted, almost spherical crystal of this type was found [$(0.1 \times 0.1 \times 0.1)$ mm³], and following data collection, the crystal structure was obtained in the cubic space group $Fd\bar{3}m$ (No. 227, origin at $\bar{3}m$). In the initial solution the 16d site ($^1/_2$, $^1/_2$, $^1/_2$) was occupied by sodium to give a Sr:In:Na ratio of 6:4:2. This ratio was not supported by the microprobe analysis (vide infra) which, instead, suggested a Sr:In:Na ratio of 6:4.3:0. Placing indium on the 16d site and allowing the 16d site occupancy to vary led to an occupancy of approximately 16% and a Sr:In ratio of 6:4.3, in good agreement with the microprobe data.

The anisotropic displacement parameters of the nitrogen atom occupying the 16c site (0,0,0) were found to be large in the direction of the body diagonal of the unit cell. The magnitude of the isotropic displacement parameter, however, was not unusually large and hence did not indicate any partial occupancy. Therefore, a split site model was used in which the nitrogen atom was moved slightly away from the 16c site to a more general 32e site (x, x, x; $x = 0.01$) but with a fixed occupancy of 50%.[49] The displacement parameter of the nitrogen atom sitting on the 8a site (1/8, 1/8, 1/8) was also unusually large. The site occupancy for this atom was also allowed to vary, and it refined smoothly and reproduc-

(42) Reynolds, T. K.; McGuire, M. A.; DiSalvo, F. J. *J. Solid State Chem.* **2004**, *177*, 2998−3006.

(43) Kittel, C. *Introduction to Solid State Physics*; John Wiley and Sons: New York, 1996.

(44) Aoki, M.; Yamane, H.; Shimada, M.; Sekiguchi, T.; Hanada, T.; Yao, T.; Sarayama, S.; DiSalvo, F. J. *J. Cryst. Growth* **2000**, *218*, 7−12.

(45) Kowach, G. R.; Lin, H. Y.; DiSalvo, F. J. *J. Solid State Chem.* **1998**, *141*, 1−9.

(46) Landrum, G. A.; Glassey, W. YAeHMOP: Yet Another extended Hückel Molecular Orbital Package. YAeHMOP is freely available at http://sourceforge.net/projects/yaehmop.

(47) Liu, Q.; Hoffmann, R.; Corbett, J. D. *J. Phys. Chem.* **1994**, *98*, 9360−9364.

(48) Cordier, G.; Gudat, A.; Kniep, R.; Rabenau, A. *Angew. Chem.* **1989**, *101* (12), 1689−1695.

(49) This split position cannot be modeled by N_2^{2-} since the N−N separations in both SrN_2,[50] 1.22 Å, and in BaN_2,[51] 1.14 Å, are considerably longer than the 0.5 Å separation observed between the split sites.

(50) Auffermann, G.; Prots, Y.; Kniep, R. *Angew. Chem., Int. Ed.* **2001**, *40* (3), 547−549.

(51) Vajenine, G. V.; Auffermann, G.; Prots, Y.; Schnelle, W.; Kremer, R. K.; Simon, A.; Kniep, R. *Inorg. Chem.* **2001**, *40*, 4866−4870.

ibly to 46%. These details lead to the stoichiometry Sr_6-$In_{4.32}N_{2.47}$ with R1 = 0.040 and wR2 = 0.075 for all data. The program ADDSYM[37] was used to check for higher symmetry, but none was found and, at this point, the atomic coordinates found were standardized with STRUCTURE TIDY[52] and used as the starting model for the subsequent Rietveld refinement of the neutron diffraction pattern. Details of the X-ray crystal structure refinement, atomic coordinates, and the anisotropic displacement parameters of this partial model are shown in the Supporting Information, Tables S2−S4, respectively. An ORTEP[53] representation is also shown in Figure S1 of the Supporting Information.

Semiquantitative electron microprobe spectroscopy was used to ascertain the Sr:In ratio. The average of nine readings taken from the flat faces of suitable crystals showed only the presence of strontium and indium in the ratio of Sr:In = 1.37 ± 0.17, in good agreement with that expected from the X-ray single-crystal structure (Sr:In = 1.39). No sodium peaks were observed either in energy dispersive or in wavelength dispersive mode. In addition, wavelength dispersive analysis revealed the presence of nitrogen, but a small signal was also observed for oxygen. The magnitude of the oxygen peak was typical of a small amount of surface oxidation of the highly air and moisture sensitive $Sr_6In_4(In_{0.32}Li_{0.92})N_{2.49}$ crystals.

Despite the good agreement between the single-crystal X-ray data and electron microprobe analysis, there were still two questions that needed answering. The first is the partial occupancies of the indium 16d site, the nitrogen 32e/16c site, and the nitrogen 8a site (as noted in Table S3). Partial occupancies or unusual displacement parameters can be indicative of poor absorption corrections. $Sr_6In_4(In_{0.32}Li_{0.92})$-$N_{2.49}$ has a large absorption coefficient of $\mu = 28$ mm^{-1} for Mo Kα radiation. The program SADABS[34] was used to correct for absorption ($R_{INT} = 0.0556$), and because of the almost-spherical shape of the crystal, it is expected that it will be well modeled. An analytical face-indexed absorption correction is superior to this, but due to the highly faceted nature of the crystal, this was not attempted in this case. It is very unusual or perhaps suspicious for three of the five atoms to have such peculiarities with their displacement parameters/occupancies, but these exact same features were reproduced in $Ba_6In_{4.78}N_{2.72}$ (vide infra) and an analytical face-indexed absorption correction was applied in that case. Furthermore, as noted above, the Ae:In (Ae = Sr and Ba) atomic ratios resulting from the partial occupancies for both compounds are in good agreement with the elemental analysis. Therefore, while we cannot be entirely confident about the fractional occupancy of the nitrogen sites, the Sr: In ratio, i.e. the value of the occupancy of the indium 16d site, is not in question.

The second question addresses the role of lithium in the reaction. The X-ray scattering power of lithium is very small when compared to strontium and indium; furthermore, the characteristic Kα emission energies of lithium cannot be

detected by electron microprobe analysis. Therefore, neither technique can determine the presence or absence of lithium. The vapor pressure of lithium at 350 °C is approximately 10^{-3} Pa, approximately 4 orders of magnitude less than that of sodium at this temperature. Therefore, it is unreasonable to expect that all of the excess lithium could be removed via sublimation, along with the excess sodium. Thus, at the end of the reaction, much if not all of the lithium will remain in the product mass either in its elemental form or in a compound.

Neutron Diffraction. As discussed above, at this stage it was not clear whether lithium was present in the title compound. Neutron diffraction can help to answer this question because the neutron scattering factor of lithium is negative and of a magnitude more similar to that of strontium, indium, and nitrogen than their respective X-ray scattering lengths (see Supporting Information, Table S5). Inspection of the single-crystal derived unit cell reveals various possibilities for the location of the lithium. However, the most reasonable locations are either sharing the partially occupied In 16d site or being incorporated into interstices within the crystal.

The single-crystal derived unit cell and atomic parameters shown in Tables S2 and S3 (including the use of a split site model for N1) were used as the starting model in the Rietveld refinement. All system parameters, e.g. zero point error and peak shapes, unit cell parameters, and atomic coordinates, refined smoothly; however, when the occupancy of the In 16d site was allowed to vary, it fell from 16% to −0.4%. Both X-ray single crystal and electron microprobe data provide strong evidence for this site containing 16 % indium; therefore, the fact that neutrons see an overall negative scattering length for this site is strong evidence for this site being shared by both indium and lithium. Lithium was introduced into the In 16d site, the indium occupancy was fixed at 16%, and the lithium occupancy was allowed to refine. It refined smoothly to a value of approximately 45%. In the final refinement cycles, the indium occupancy was fixed at 16% and the isotropic displacement parameters of the In 32e and 16d sites were refined as a single variable. The isotropic displacement parameters of the N 32e and 8a site were also refined as a single variable, but the occupancy of the N 8a site was allowed to refine freely. Independent, isotropic displacement parameters were used for the strontium and lithium atoms. All the aforementioned details lead to a final stoichiometry of $Sr_6In_4(In_{0.32}Li_{0.92})N_{2.49}$, with the crystallographic details and atomic coordinates collected in Tables 1 and 2, respectively. The observed, calculated, and difference plots are shown in Figure 2.

$Ba_6In_{4.78}N_{2.72}$. Following the removal of the sodium by washing with liquid ammonia, the single crystals contained in the crucible were black. $Ba_6In_{4.78}N_{2.72}$ was present with two crystal habits, octahedral [maximum size $(0.4 \times 0.4 \times 0.4)$ mm^3] and as triangular platelets [$(1.0 \times 1.0 \times 0.2)$ mm^3] with a black metallic luster. A second phase, $Ba_{19}In_9N_9$, whose structure has been reported elsewhere,[17] was also present, and it formed as platelet crystals with a black metallic luster [$(1.5 \times 0.5 \times 0.2)$ mm^3].

(52) Gelato, L. M.; Parthé, E. *J. Appl. Crystallogr.* **1987**, *20*, 139−143.
(53) Farrugia, L. J. *J. Appl. Crystallogr.* **1997**, *30*, 565.

Table 1. Crystallographic Details for Sr$_6$In$_4$(In$_{0.32}$Li$_{0.92}$)N$_{2.49}$ and Ba$_6$In$_{4.78}$N$_{2.72}$[a]

param	Sr$_6$In$_4$(In$_{0.32}$Li$_{0.92}$)N$_{2.49}$	Ba$_6$In$_{4.78}$N$_{2.72}$
Z	8	8
crystal system	cubic	cubic
space group	$Fd\bar{3}m$ (origin 2) (No. 227)	$Fd\bar{3}m$ (origin 2) (No. 227)
a/Å	14.3752(4)	15.216(1)
V/Å^3	2970.58(8)	3523.3(6)
$2\theta_{max}$	148	59.82
radiation	neutrons	Mo Kα
wavelength/Å	1.5402(2)	0.710 73
temp/K	173(2)	293(2)
reflns collcd/unique	174/174	7166/282 [R(int) = 0.065]
abs corr	none (μR = 0.59)	analytical
abs/cm^{-1}	linear attenuatn factor = 1.273	μ = 192.66
struct solution/program	direct methods/SHELXS[b]	direct methods/SIR97
refinement method/program	full profile Rietveld/GSAS, EXPGUI	full-matrix least squares on F^2/SHELX
goodness of fit	χ^2 = 1.062	1.181 (on F^2)
final R indices	R$_{wp}$ = 0.0550, R$_p$ = 0.0451, R(F^2) = 0.1746	$I > 2\sigma(I)$: R1 = 0.0238, wR2 = 0.0530
final R indices	bckgrd subtracted: wR$_p$ = 0.0527, R$_p$ = 0.0488	all data: R1 = 0.0291, wR2 = 0.0545
largest diffractn peak and hole/e Å^{-3}	n/a	0.912/−1.118

[a] The different R values are defined in the Supporting Information. Note that the absorption coefficient of Ba$_6$In$_{4.78}$N$_{2.72}$ is expressed in units of cm^{-1}. [b] Used in the initial single-crystal X-ray analysis.

Table 2. Atomic Coordinates and Isotropic Displacement Parameters (10^3 Å^2) for Sr$_6$In$_4$(In$_{0.32}$Li$_{0.92}$)N$_{2.49}$ and, Shown in Italics, for Ba$_6$In$_{4.78}$N$_{2.72}$ (Both in Space Group $Fd\bar{3}m$, Origin 2 (Origin at $\bar{3}m$)[a]

atom	Wyckoff positn	x	y	z	100U_{iso} or U_{eq}	occ
Sr1	48f	0.31008(6)	0.125	0.125	13.3(6)	1
Ba1	*48f*	*0.30796(4)*	*0.125*	*0.125*	*31.6(2)*	*1*
In1	32e	0.30044(2)	0.30044(2)	0.30044(2)	9(1)	1
In1	*32e*	*0.30278(2)*	*0.30278(2)*	*0.30278(2)*	*24.1(2)*	*1*
In2	16d	0.5	0.5	0.5	9(1)	0.16
Li1	16d	0.5	0.5	0.5	15(13)	0.46(6)
In2	*16d*	*0.5*	*0.5*	*0.5*	*25.8(9)*	*0.389(5)*
N1	32e	0.0114(2)	0.0114(2)	0.0114(2)	13(1)	0.5
N1	*32e*	*0.0111(9)*	*0.0111(9)*	*0.0111(9)*	*40(7)*	*0.5*
N2	8a	0.125	0.125	0.125	13(1)	0.49(1)
N2	*8a*	*0.125*	*0.125*	*0.125*	*50(13)*	*0.72(8)*

[a] The results for Sr$_6$In$_4$(In$_{0.32}$Li$_{0.92}$)N$_{2.49}$ are from the Rietveld refinement of powder neutron data; those for Ba$_6$In$_{4.78}$N$_{2.72}$, from single crystal X-ray studies. For Ba$_6$In$_{4.78}$N$_{2.72}$, the equivalent isotropic displacement parameter, U_{eq}, is defined as one-third of the trace of the orthogonalized $\mathbf{U}_{ij}$ tensor.
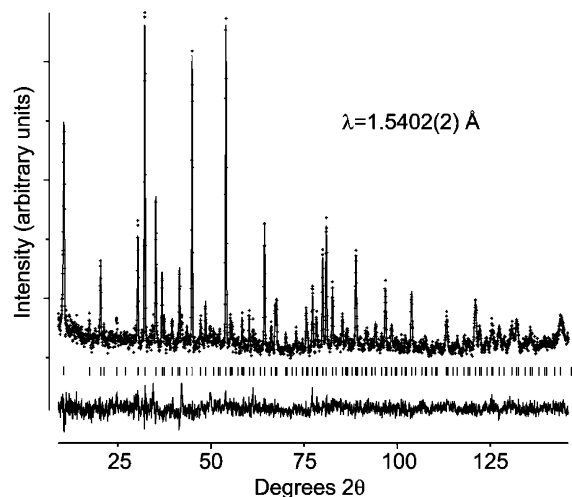

Figure 2. Observed (crosses), calculated (line), and difference plots for the full profile Rietveld refinement of Sr$_6$In$_4$(In$_{0.32}$Li$_{0.92}$)N$_{2.49}$. The high level of background noise is due mainly to the large absorption and incoherent neutron cross sections of indium. At 150° in 2θ, the resolution is 0.8 Å.

Single crystals for X-ray diffraction were selected from the products in an argon-filled glovebox and sealed in glass capillaries under argon since the single crystals were not stable in air. The crystals of Ba$_6$In$_{4.78}$N$_{2.72}$ were solved in space group $Fd\bar{3}m$ (No. 227, origin at $\bar{3}m$) by direct methods;[54] the crystallographic details and atomic coordinates are shown in Tables 1 and 2, respectively. A table and ORTEP[53] representation of the anisotropic displacement parameters can be found in the Supporting Information, Tables S6 and Figure S2, respectively. Inspection of the Fourier difference map again indicated evidence that the N1 atom should be modeled as a split site. There was no effect on the R value and residuals when the N1 atom was moved from the 16c site to the 32e site with 50% occupancy [R1-(all data) = 0.0291 in both cases]. However, the displacement parameter, U_{iso}, halved to 0.040(7) from 0.078(8) Å^2. Following these steps in the refinement, it was noticed that the displacement parameter of the N2 (8a site) was unusually large [0.09(1)], and therefore, the site occupancy was allowed to vary. It refined smoothly to a final value of 72%, and U_{iso} dropped to 0.05(1) Å^2.

The single-crystal results lead to a Ba:In ratio of 6:4.78, and in support of this stoichiometry, the Ba:In ratios found by ICP for two samples of hand-picked single crystals of Ba$_6$In$_{4.78}$N$_{2.72}$ were 6:4.83 and 6:4.87, in reasonable agreement with each other. This compound was made without the presence of lithium, and therefore, there is no reason to believe that lithium is incorporated. A reaction between

(54) Altomare, A.; Burla, M. C.; Camalli, M.; Cascarano, G. L.; Giacovazzo, C.; Guagliardi, A.; Moliterni, A. G. G.; Polidori, G.; Spagna, R. *J. Appl. Crystallogr.* **1999**, *32*, 115−119.
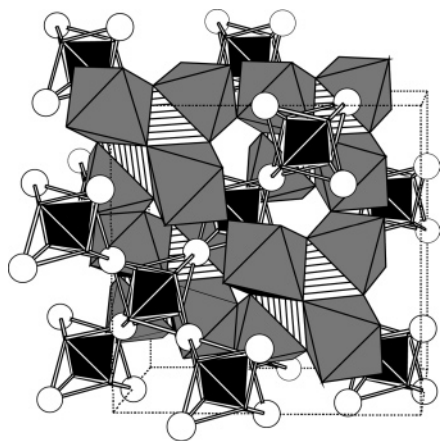
Figure 3. Hypothetical Ae_2In_2N unit cell. In1 atoms are at the apices of the tetrahedra, and the In2 atoms are shown as white spheres. Ae atoms form the corner of the gray (N1 centered) and hatched (N2 centered) octahedra.

Table 3. Important Interatomic Separations in $Sr_6In_4(In_{0.32}Li_{0.92})N_{2.49}$ and $Ba_6In_{4.78}N_{2.72}{}^a$

interactn	$Sr_6In_4(In_{0.32}Li_{0.92})N_{2.49}$	$Ba_6In_{4.78}N_{2.72}$
Ae−N1(16c)	2.6806(3)	2.8308(3)
Ae−N1(32e)	2.543(15), 2.833(18)	2.667(13), 3.014(16)
Ae−N2(8a)	2.6572(8)	2.7841(6)
Ae−In1	3.5649(5), 3.7684(8)	3.8265(8), 4.0364(7)
Ae−In2	3.7252(6)	3.9717(6)
Ae−Ae	3.7578(12)	3.9373(9)
In1−In1 (intratetrahedral)	3.0277(1)	3.1084(14)
In1−In2 (or Li)	3.046(1)	3.2088(4)
N1(16c)−In1	4.433(1)	4.745(1)
N1(32e)−In1	4.346(1), 4.531(1)	4.655(1), 4.848(1)
N2−In1	4.362(1)	4.686(1)
N1(16c)−N2	3.108(1)	3.294(1)
N1(32e)−N2	2.825(1), 3.392(1)	3.003(1), 3.586(1)

^{a} Note that, in both $Sr_6In_4(In_{0.32}Li_{0.92})N_{2.49}$ and $Ba_6In_{4.78}N_{2.72}$, the N1 atom does not occupy the 16c site (0, 0, 0); rather, it occupies the 32e site (0.01, 0.01, 0.01) with 50% occupancy.

lithium, barium, indium, and nitrogen in a sodium flux was not attempted.

Structure Description. $Sr_6In_4(In_{0.32}Li_{0.92})N_{2.49}$ and $Ba_6In_{4.78}N_{2.72}$ are isostructural and have partial occupancy on the same atomic sites. The major difference between them is that in $Sr_6In_4(In_{0.32}Li_{0.92})N_{2.49}$ the 16d site is statistically occupied by both indium and lithium but in $Ba_6In_{4.78}N_{2.72}$ it is fractionally occupied only by indium. Shown in Figure 3 is the structure of the hypothetical compound $Ae_6In_6N_3$ or Ae_2In_2N (Ae = alkaline earth), which is the parent structure for both $Sr_6In_4(In_{0.32}Li_{0.92})N_{2.49}$ and $Ba_6In_{4.78}N_{2.72}$. The structure is drawn in a manner that emphasizes the two distinct subnets that can be visualized in the compound, the network of In (and Li) and of Ae−N (Ae = Sr or Ba). The N1 (32e site) and N2 (8a site) centered octahedra are shown with different shading. In the subsequent discussion of "Ae_2In_2N", the N1 atom is placed on its nonsplit average position, the 16c site. Important interatomic distances in "Ae_2In_2N", including those from the 16c site (the average N1 site), are shown in Table 3. The coordination geometries of the Ae, In1, and In2 atoms are shown in the Supporting Information, Figure S3. The structure shown in Figure 3 is very close to the η-carbide structure type, the only difference being that both alkaline earth octahedra are at least partially centered

by nitrogen; in the η-carbide structure type, only the 16c site is occupied.

The indium or indium−lithium subnet is a three-dimensional network of corner-sharing stellae quadrangulae, or tetracapped tetrahedra. The inner tetrahedra are formed from the In 32e site and are, in both compounds, fully occupied. The capping 16d site is partially occupied by either lithium and indium [$Sr_6In_4(In_{0.32}Li_{0.92})N_{2.49}$] or indium ($Ba_6In_{4.78}N_{2.72}$). As can be seen from Table 3, the intratetrahedral indium separations (32e−32e site distance) are shorter than the capping-tetrahedral indium separations (32e−16d site distance) in both compounds.

All the near-neighbor indium−indium distances in $Sr_6In_4(In_{0.32}Li_{0.92})N_{2.49}$ and $Ba_6In_{4.78}N_{2.72}$ are shorter than 3.25 Å, the nearest neighbor distance in indium metal, and compare well to the indium−indium separations in (the nonisostructural compounds) $SrIn_2{}^{[55]}$ and $BaIn_2.{}^{[55]}$ In $SrIn_2$ and $BaIn_2$, the four indium−indium separations range from 2.98 to 3.30 Å and from 2.97 to 3.12 Å, respectively. In $Sr_6In_4(In_{0.32}Li_{0.92})N_{2.49}$, the indium−lithium interactions created by the mixed occupancy of the 16d site lead to indium−lithium separations of 3.04 Å. This compares well to the indium−lithium separations in $Li_3In_2{}^{[56]}$ that range from 2.85 to 3.43 Å, with a mean value of 3.16 Å. Mixed lithium−indium site occupancy has been observed before in the binary compound LiIn, which has a wide composition range that, although relatively ill-defined,[57] extends over ca. 2 at. % at 100 °C and from 47 to 63 at. % at 415 °C, indicating mixed site occupancy at relatively low temperatures.

An indium or indium−lithium, stellar quadrangular network has, as far as the authors can tell, not been previously reported; furthermore, isolated indium tetrahedra are also rare within extended structures. According to the Zintl concept, an isolated In_4 tetrahedra would be expected to have a charge of 8− and $In_4{}^{8-}$ tetrahedra are indeed observed within the binary compound Na_2In,[58] but to our knowledge, there is only one further extended structure type that is able to support the $In_4{}^{8-}$ cluster, namely, $Ae_{19}In_8N_7{}^{[12]}$ (Ae = Ca and Sr). Molecular In_4 species are also rare, but in the past decade compounds such as $In_4[C(SiMeRR')_3]_4{}^{[59]}$ have been successfully synthesized. The molecules contain an In_4 tetrahedral core in which every vertex is ligated. Indium−indium bond lengths are typically 3.00 Å in the molecular compounds and range from 3.07 to 3.15 Å in Na_2In, in good agreement with that found here.

The basis of the $Ae_{6/3}N$ subnet is a supertetrahedron that consists of five, face-sharing octahedra. This unit can be observed in Figure 4, and it can be seen that each Ae atom of the central octahedron is shared by three nitrogen atoms. The central, hatched octahedron is ideal but the four

(55) Nuspl, G.; Polborn, K.; Evers, J.; Landrum, G. A.; Hoffmann, R. *Inorg. Chem.* **1996**, *35*, 6922−6932.
(56) Stöhr, J.; Schäfer, H. *Z. Naturforsch.* **1979**, *B34*, 653−656.
(57) *Binary Alloy Phase Diagrams*, 2nd ed.; ASM International: Materials Park, OH; Plus Updates, Version 1.
(58) Sevov, S. C.; Corbett, J. D. *J. Solid State Chem.* **1993**, *103*, 114−130.
(59) Uhl, W.; Jantschak, A.; Saak, W.; Kaupp, M.; Wartchow, R. *Organometallics* **1998**, *17*, 5009−5017.
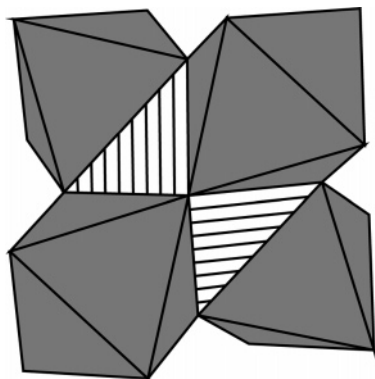
Figure 4. Supertetrahedron comprising four N1-centered distorted octahedra and one N2-centered ideal octahedron.

neighboring octahedra (solid color) are slightly distorted. The supertetrahedra share corners to build up a diamond-like net in which all octahedra share faces and all nitrogen atoms continue to be shared by three alkaline earth atoms.

Within the alkaline earth octahedra, there are two distinct sites for nitrogen occupation, the 16c (N1) and 8a (N2) sites. The 16c and 8a nitrogen atoms reside in the slightly distorted and ideal octahedra, respectively. As shown in Table 3, the interatomic spacing from the 8a site to the Ae site is shorter than the distance from the 16c site to the Ae site. However, in both $Sr_6In_4(In_{0.32}Li_{0.92})N_{2.49}$ and $Ba_6In_{4.78}N_{2.72}$, the nitrogen atom in 16c site shifts to the more general 32e site of (x, x, x; $x = 0.01$), which results in the generation of the two sets of three Ae—N1 distances detailed in Table 3. One set of these Ae—N1 distances is shorter than the Ae—N2 distance and the other is longer, but all the Ae—N separations detailed in Table 3 compare well to those found in Sr_2N and Ba_2N, which have Sr—N or Ba—N distances of 2.61 and 2.76 Å.[60]

It is postulated that the shift of the N1 atom from the 16c to the 32e site is in response to the presence or absence of the neighboring N2 atom; the 16c and 8a sites are separated by only 3.11 Å in $Sr_6In_4(In_{0.32}Li_{0.92})N_{2.49}$ and 3.29 Å in $Ba_6In_{4.78}N_{2.72}$. Such a Coulombic repulsion between the nominally highly charged N^{3-} anions has been observed before in the compound $Na_{14}Ba_{14}CaN_6$.[61] This compound contains the cluster $Ba_{14}CaN_6$, which is a fragment of a cubic close packed layer of cations with nitrogen in the six octahedral holes. An equally valid representation of the $Ba_{14}CaN_6$ cluster is of a superoctahedron formed by the edge-sharing of six, nitrogen-centered Ba_5Ca octahedra—the calcium atom is shared by all six octahedra and is at the center of the close packed layer. The octahedral holes within this cluster that are occupied by the N^{3-} are in close proximity to one another, and to minimize repulsion between the closed shell anions, they are observed to have radially "breathed out" from the central calcium cation to create inter-nitrogen separations of 3.64 Å.

An interesting comparison can be made by comparing how the interatomic separations differ between $Sr_6In_4(In_{0.32}Li_{0.92})$-$N_{2.49}$, which has a smaller unit cell, and $Ba_6In_{4.78}N_{2.72}$, which

(60) Reckeweg, O.; DiSalvo, F. J. *Solid State Sci.* **2002**, *4*, 575−584.
(61) Steinbrenner, U.; Simon, A. *Angew. Chem., Int. Ed. Engl.* **1996**, *35* (5), 552−554.

has a larger unit cell. The increase in the unit cell size is due to the larger size of the alkaline earth cation, leading to the observed expansion within the Ae−N sublattices. However, for the structure of the two subnets to remain commensurate, there must also be an expansion within the indium sublattice, and by inspection of Table 3, it can be seen that the majority of this expansion occurs in the separation between the capping, 16d, site and the tetrahedral, 32e, site rather than between the indium atoms within the tetrahedra: the difference between the intratetrahedral distance in Sr_6-$In_4(In_{0.32}Li_{0.92})N_{2.49}$ and in $Ba_6In_{4.78}N_{2.72}$ is only 0.08 Å, which is smaller than 0.17 Å, the comparable difference between the capping, 16d, site and the tetrahedral, 32e, site, in the two title compounds. This suggests that the intratetrahedral bonding is more important than the capping-tetrahedral bonding (q.v. The Indium or Indium/Lithium Network in the Supporting Information).

The final comparison to be made is that between the two subnets. The separation between the Ae−N and In (and Li) subnets also increases with the replacement of strontium by barium, but in both $Sr_6In_4(In_{0.32}Li_{0.92})N_{2.49}$ and $Ba_6In_{4.78}N_{2.72}$, the Ae−In (Ae = Sr and Ba) separations are longer than those found in, for example, $SrIn_2$[55] (6 × 3.33 Å) and $BaIn_2$[55] (6 total, ranging from 3.53 to 3.87 Å). This inconsistency emphasizes the separation of ionic and covalent bonding that can be visualized in these compounds; i.e., of primary concern to the Ae−N and In(Li) networks is the intra-subnet bonding rather than the inter-subnet bonding.

All the above results have established the actual stoichiometries of the title compounds to be $Sr_6In_4(In_{0.32}Li_{0.92})N_{2.49}$ and $Ba_6In_{4.78}N_{2.72}$. At this point it is worth noting that, despite the stoichiometric differences, the excess electron count for the two compounds is, within experimental error, the same; i.e., on the basis of valence electron counts derived from "expected" oxidation states, $Sr_6In_4(In_{0.32}Li_{0.92})N_{2.49}$ can be written as $(Sr^{2+})_6(In^{3+})_{4.32}(Li^+)_{0.92}(N^{3-})_{2.49}(e^-)_n$ and Ba_6-$In_{4.78}N_{2.72}$ can be written as $(Ba^{2+})_6(In^{3+})_{4.78}(N^{3-})_{2.72}(e^-)_n$, where $n = 18.4$ and 18.2, respectively. Such a similarity between electron counts suggests that there is an electronic "explanation" for these stoichiometries, and to that we now turn.

Extended Hückel Calculations. To understand the partial occupancies of $Sr_6In_4(In_{0.32}Li_{0.92})N_{2.49}$ and $Ba_6In_{4.78}N_{2.72}$, extended Hückel calculations were carried out with the program YAeHMOP.[46] As mentioned above, the parent structure of both phases is the hypothetical compound Ae_2-In_2N (Ae = Sr and Ba) whose primitive unit cell contains 30 atoms, distributed as either $Sr_{12}In_8(In,Li)_4N_4N_2$ or Ba_{12}-$In_8In_4N_4N_2$, where the two sites that exhibit partial occupancy in the experimental structures are highlighted with italics. The partially occupied indium (and lithium) site is the 16d site that caps the faces of the In_4 tetrahedra. For ease of discussion throughout this section, the stoichiometry of both the experimental and theoretical compounds will be written in terms of the population of the primitive unit cell; for example, $Sr_6In_4(In_{0.32}Li_{0.92})N_{2.49}$ will be written as Sr_{12}-$In_8(In_{0.64}Li_{1.84})N_{4.98}$ and Ae_2In_2N as $Ae_{12}In_8In_4N_4N_2$.

Our view of the title compounds is one based upon the decomposition of the hypothetical crystal structure of Ae_{12}-$In_8In_4N_4N_2$ into a covalent indium/lithium network and a predominantly ionic alkaline-earth−nitrogen network. This viewpoint suggests that the electronic requirements of Ae_{12}-$In_8In_4N_4N_2$ can be expressed as the sum of the electronic requirements of each subnet. To a first approximation, the electronic requirements of the predominantly ionic alkaline-earth−nitrogen subnet are straightforward; the alkaline earth atoms will formally become fully oxidized and the nitrogen atoms will formally become fully reduced, creating Ae^{2+} and N^{3-} ions.

The electronic requirements of the partially complete stellar quadrangular subnet are not so clear but are developed within the Supporting Information. It is shown that the electronic requirements of the partially complete stellar quadrangular subnet of both $Ba_6In_{4.78}N_{2.72}$ and $Sr_6In_4(In_{0.32}$-$Li_{0.92})N_{2.49}$ can be expressed as 20 valence electrons/inner In_4 tetrahedron, irrespective of the number of indium or lithium atoms occupying the capping 16d site. Indeed, the occupation of the capping 16d site by indium or lithium serves merely to modify the electron count of the stellar quadrangular subnet because no new bonding states are introduced; i.e., the central In_4 tetrahedron sets the number of bonding crystal orbitals, into which the capping atoms' orbitals are assimilated.[62]

The electronic requirements of the two subnets within Ae_v-$In_wIn_xN_yN_z$ have been stated, and just as the complete crystal structure of $Ae_vIn_wIn_xN_yN_z$ is the sum of the two subnets, it is suggested that the electronic requirements of the generic compound $Ae_vIn_wIn_xN_yN_z$ is the sum of the valence electron requirements of each subnet; i.e., 20e⁻/inner tetrahedron + 8e⁻/nitrogen atom. Our hypothesis is that the fractional/mixed occupancies of the 16d and 8a site act in a coordinated fashion to optimize the bonding within $Ba_6In_{4.78}N_{2.72}$ and Sr_6-$In_4(In_{0.32}Li_{0.92})N_{2.49}$. A test of this hypothesis is contained in Figure 5, which shows the COOP analysis of the partially complete stellar quadrangular subnets of the compounds Sr_{12}-$In_8(InLi_2)N_5$ and $Ba_{12}In_8In_2N_5$. Both Sr_{12}-$In_8(InLi_2)N_5$ and $Ba_{12}In_8In_2N_5$ contain five nitrogen atoms and two inner tetrahedra/primitive cell, suggesting a required electron count of 80 valence electrons/primitive cell. As shown in Figure 5, the transition from bonding to antibonding interactions within the stellar quadrangular subnet was indeed found to occur at 80 valence electrons in the primitive cell.

Figure 5a,b demonstrates the validity of our model for the hypothetical compounds $Sr_{12}In_8(InLi_2)N_5$ and $Ba_{12}In_8In_2N_5$, which represent the closest possible matches to the experimental compounds, $Sr_{12}In_8(In_{0.64}Li_{1.84})N_{4.98}$ and $Ba_6In_{4.78}N_{2.72}$. However, the stoichiometries of the hypothetical and experimental compounds are different, e.g. $Sr_{12}In_8(In_{0.64}Li_{1.84})$-$N_{4.98}$ vs $Sr_{12}In_8(InLi_2)N_5$. Within our calculations, symmetry can be lowered by removing symmetry-equivalent atoms but
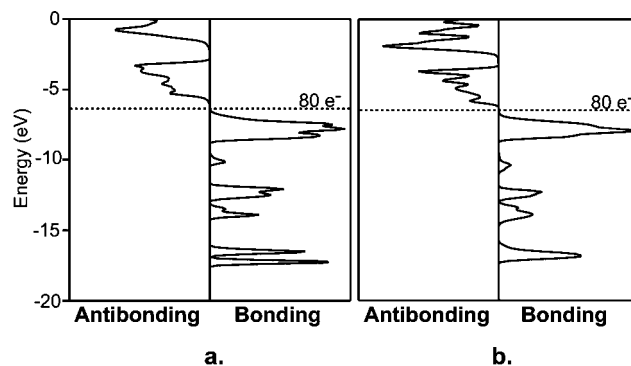

Figure 5. COOP analyses of the partially complete stellar quadrangular networks of (a) $Sr_{12}In_8In_1Li_2N_5$ and (b) $Ba_{12}In_8In_2N_5$. According to our model, the stellar quadrangular subnet and the five nitrogen atoms each require 40 valence electrons/primitive cell, giving a total requirement of 80 valence electrons/primitive cell. As shown, the transition from bonding to antibonding within the stellar quadrangular network indeed occurs at 80 valence electrons/primitive cell.

partial occupancy of a single site is not possible. Therefore, we cannot exactly model the electronic structure at the exact stoichiometries of the title compounds. However, the strength of the model we have built up is that it can take into account partial occupancies in both the nitrogen and capping atom sites. For example, according to our hypothesis, the required valence electron count of $Sr_{12}In_8(In_{0.64}Li_{1.84})N_{4.98}$ is 40 + $(4.98 \times 8) = 79.84$ valence electrons/primitive cell and that of $Ba_{12}In_8In_{1.56}N_{5.44}$ is 40 + $(5.44 \times 8) = 83.52$ valence electrons/primitive cell: the partial occupancies have not prohibited us from calculating the number of electrons required to fulfill the electronic requirements of each compound.

Do the experimental and calculated electron counts match? If it is assumed that lithium, strontium, barium, indium, and nitrogen have 1, 2, 2, 3, and 5 valence electrons each, the number of valence electrons within the primitive cells of Sr_{12}-$In_8(In_{0.64}Li_{1.84})N_{4.98}$ and $Ba_{12}In_8In_{1.56}N_{5.44}$ is 76.7(4) and 79.9-(9), respectively. Both these values are approximately three electrons short of attaining the expected magic electron count. This small deviation arises because we have oversimplified the bonding within the alkaline-earth−nitrogen subnet. Our viewpoint was that this was a completely ionic network whose electronic structure would consist of a set of mainly nitrogen p bonding states well below the Fermi energy and a set of mainly alkaline-earth s antibonding states well above the Fermi energy. Such a wide separation of bonding and antibonding levels would be insensitive to the position of Fermi energy; however, the bonding within nitrides always has considerable covalent character. The effect of this covalent character is to distribute the antibonding states of the alkaline-earth−nitrogen network both above, around and below the Fermi energy. In fact, as shown in Figure S9 of the Supporting Information, an antibonding interaction is present at the Fermi energy; therefore, the observed electron count in $Sr_{12}In_8(In_{0.64}Li_{1.84})N_{4.98}$ and $Ba_{12}In_8In_{1.56}N_{5.44}$ is the result of the attempts to maximize the bonding of both the stellar quadrangular and the alkaline-earth−nitrogen subnets.

Band Structure and Density of States. Shown in Figure 6 is the calculated band structure and total density of states

(62) This result that capping atoms have no effect on optimal electron count is very similar to the capping principle outlined by Mingos and Wales.[63]

(63) Mingos, M. P.; Wales, D. J. *Introduction to Cluster Chemistry*; Prentice Hall: Englewood Cliffs, NJ, 1990.
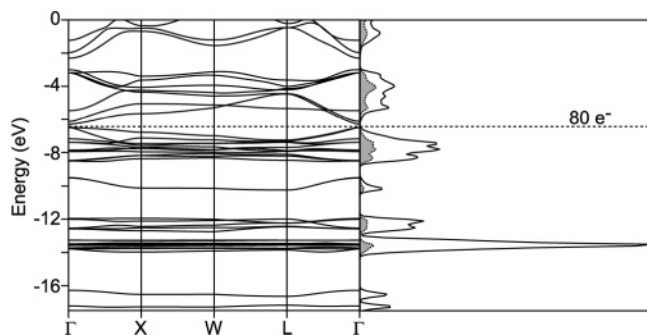
Figure 6. Calculated band structure and total density of states (DOS) of $Sr_{12}In_8In_1Li_2N_5$. Shown in gray is the projected density of states of the strontium atoms. A total of 80 valence electrons/primitive cell fulfills the bonding requirements of the stellar quadrangular subnet in $Sr_{12}In_8In_1Li_2N_5$ and is also found to completely fill up all the bands below approximately -6 eV. The sharp peak in the DOS centered at approximately -13.8 eV is formed primarily from nitrogen 2p bands; all the other peaks below -6 eV are predominantly indium in character.
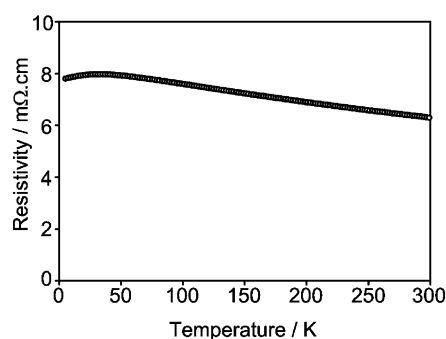
Figure 7. Measured resistivity of a pressed pellet of $Sr_6In_4(In_{0.32}Li_{0.98})$-$N_{2.49}$.

(DOS) of the hypothetical compound $Sr_{12}In_8(InLi_2)N_5$. A small gap in the DOS is apparent at ca. -6.5 eV, and as labeled, this corresponds to 80 valence electrons/primitive cell or, more precisely, 40 valence electrons for the stellar quadrangular network and 40 valence electrons for the five nitrogen atoms. Figure 6 suggests, therefore, that if the required valence electron count were fulfilled in $Sr_{12}In_8(In_{0.64}Li_{1.84})N_{4.98}$ and $Ba_{12}In_8In_{1.56}N_{5.44}$, then semiconducting behavior would be expected for both compounds. However, both compounds have been oxidized, which lowers the Fermi energy into the bands centered at approximately -8 eV, and, instead, metallic behavior would be expected for Sr_{12}-$In_8(In_{0.64}Li_{1.84})N_{4.98}$ and $Ba_{12}In_8In_{1.56}N_{5.44}$.

Shown in gray in Figure 6 are the projected density of states of the strontium atoms. There is strontium character in almost all the bands; the 20 e^-/tet rule derived from the inner tetrahedra of the stellar quadrangular network is maintained despite significant interactions with its neighboring, interpenetrating, predominantly ionic network.

Electrical Resistivity. The measured resistivity of a pressed pellet of $Sr_6In_4(In_{0.32}Li_{0.92})N_{2.49}$ is shown in Figure 7, and because of possible scattering from grain boundaries and voids in the pellet, these data represent an upper limit to the actual resistivity of $Sr_6In_4(In_{0.32}Li_{0.92})N_{2.49}$. The powder XRD pattern of the pellet taken after the measurements did not show any noticeable difference in the positions or intensities of the Bragg peaks, and furthermore, no new peaks

had appeared; i.e., according to X-ray analysis, the pellet did not decompose or oxidize during the measurement.

The resistivity shown in Figure 7 decreases slightly with increasing temperature but not by a significant amount; the trend is essentially flat, the resistivity varying from 7.8 mΩ·cm at 5 K to 6.3 mΩ·cm at 299 K. This is approximately 3 orders of magnitude more resistive than copper and 1 order of magnitude more resistive than Kanthal wire, the high-resistivity alloy used in some electric furnaces.

The resistivity data for $Sr_6In_4(In_{0.32}Li_{0.92})N_{2.49}$ are consistent with a highly defective, high carrier concentration metal, which is also consistent with the metallic behavior suggested by extended Hückel calculations but with low mobility carriers. The low mobility is due to random partial occupancies in $Sr_6In_4(In_{0.32}Li_{0.92})N_{2.49}$ which produce considerable disorder scattering. The concentration of partial and mixed occupancies does not depend on temperature, and hence, a flat, relatively high resistivity vs temperature behavior is expected. The data for Figure 7 are also consistent with a degenerately doped semiconductor, and as neither the highly pure reagents nor the clean-room environment required for highly pure semiconductor fabrication were employed, it is also possible that $Sr_6In_4(In_{0.32}Li_{0.92})N_{2.49}$ is a semiconductor with a small quantity of impurity carriers.

Conclusion. Two new indium nitrides have been synthesized and characterized. Like all other ternary indium nitrides of this class, their structures can be visualized in terms of interpenetrating nets, one ionic and the other covalent in bonding character. Considerable partial and/or mixed occupancies are present in both compounds. Even though the stoichiometries are different in $Sr_6In_4(In_{0.32}Li_{0.92})N_{2.49}$ and $Ba_6In_{4.78}N_{2.72}$, they are electronically similar and the electron count in both compounds is the result of attempts to optimize the bonding requirements of the subnets of both compounds. $Sr_6In_4(In_{0.32}Li_{0.92})N_{2.49}$ is found to have a room-temperature resistivity of 6.3 mΩ·cm, with a weak temperature dependence.

Supporting Information Available: A table of H_{ij} and ζ_1 values used in the electronic structure calculations, Table S1; single-crystal

X-ray crystal structure refinement data, atomic coordinates, and anisotropic displacement parameters of the partial model, Sr_6-$In_{4.32}N_{2.47}$, Tables S2−S4; an ORTEP representation of the anisotropic displacement parameters of $Sr_6In_{4.32}N_{2.47}$, Figure S1; definition of crystallographic R values, a table of neutron cross sections, Table S5; a table and ORTEP representation of the anisotropic displacement parameters of $Ba_6In_{4.78}N_{2.72}$, Table S6 and Figure S2, respectively; the coordination environments of the Ae, In1, and In2 atoms, Figure S3; the development of the electronic requirements of the stellar quadrangular networks of $Sr_6In_4(In_{0.32}Li_{0.92})N_{2.49}$ and $Ba_6In_{4.78}N_{2.72}$; the COOP analysis of the alkaline-earth−nitrogen network in $Sr_{12}In_8In_1Li_2N_5$, Figure S9; an input file used for YAeHMOP, including the primitive unit cell and atomic coordinates; and crystallographic information files (CIF) for $Sr_6In_4(In_{0.32}$-$Li_{0.92})N_{2.49}$ and $Ba_6In_{4.78}N_{2.72}$. This material is available free of charge via the Internet at http://pubs.acs.org. The CIF files are also deposited at the Fachinformationzentrum Karlsruhe, D-76344 Eggenstein-Leopoldshafen, Germany, with depository numbers 415294 [$Sr_6In_4(In_{0.32}Li_{0.92})N_{2.49}$] and 415293 ($Ba_6In_{4.78}N_{2.72}$).

IC050613I